COBEM 2021 26th International Congress of Mechanical Engineering
November 22-26, 2021, Virtual Congress, Brazil

COB-2021-2042
COMPARISON OF SLURRY JET EROSION BEHAVIOUR OF THERMAL SPRAY COATINGS WITH DIFFERENT LEVELS OF HARDNESS

André Chicoski
Universidade Federal do Paraná – UFPR. Av. Cel. Francisco Heráclito dos Santos, S/N, Bloco IV do Setor de Tecnologia, Centro Politécnico da UFPR. Jd. das Américas, Curitiba, PR.
andrechicoski@gmail.com

Ramón Sigifredo Cortés Paredes
Universidade Federal do Paraná – UFPR. Av. Cel. Francisco Heráclito dos Santos, S/N, Bloco IV do Setor de Tecnologia, Centro Politécnico da UFPR. Jd. das Américas, Curitiba, PR.
ramon@ufpr.br

Gustavo Bavaresco Sucharski
Instituto de Tecnologia para o Desenvolvimento – Lactec. Av. Pref. Lothário Meissner 01. Jd. Botânico. Curitiba, PR.
gustavo.sucharski@lactec.org.br

Anderson Geraldo Marenda Pukasiewicz
Universidade Tecnológica Federal do Paraná – UTFPR, Campus Ponta Grossa. R. Dr. Washington Subtil Chueire, S/N. Jd. Carvalho. Ponta Grossa, PR.
anderson@utfpr.br

Abstract. *Currently in Brazil, more than 60 % of electric energy comes from hydro generation. In hydroelectric generation, some mechanical components are often exposed to wear phenomena, usually cavitation and/or solid particle erosion. The use of coatings is an alternative to reduce the wear and, in this scenario, thermal spray technology appears as a relevant solution with minimum or no impact to the component substrate. Regarding solid particle erosion, it is usual the application of hard coatings like martensitic steels or chromium/tungsten carbides. In this work, two wear-resistant commercial alloys, with different levels of hardness, were applied on carbon steel substrate by Arc Spray Process (ASP) and subjected to slurry jet tests with constant parameters. The influence of surface finishing – using single-step sanding or full polishing – on the wear rates was also verified. The results indicated that the coating behaviour tends to be similar to that expected for bulk materials, in which, for incidence angle of 90 °, the wear rate is bigger for harder alloys. Scanning Electron Microscope (SEM) analysis of the eroded surfaces showed different wear mechanisms according to the hardness of the coating: microploughing and microcutting effects for softer material and microcracking and fragile fracture for harder material. The surface finishing – sanding and polishing – reduced the initial wear rates for both alloys, however, it did not compensate for the mass loss caused by the finishing processes themselves.*

Keywords: *erosion, thermal spray, slurry jet, coating*

1. INTRODUCTION

The Brazilian power generation is based on renewable source, which represents 83% of the country's energy matrix. In this context, hydro generation has the most important role with more than 109 GW of installed capacity, representing 62% of the matrix (ANEEL, 2021).

For the transformation of hydraulic energy into electricity, the hydroelectric powerplants use turbines which design depends on a number of parameters, in special the head, that indicates the elevation of water levels between the reservoir and the downstream (MOURA; MOURA; ROCHA, 2019). Based on this information, the type of turbine wheel is selected: Pelton type for high heads, Francis for medium heads and Kaplan or bulb for reduced heads (MULLER, 2010). Each model, therefore, works exposed to different water flows and pressures.

Regardless of the turbine model, the wheels are often exposed to wear phenomena like cavitation and solid particle erosion. The first is related to the formation of vapor bubbles along the liquid water and it is related to the machine design, such as downstream level and profile of the rotor blades (MOURA; MOURA; ROCHA, 2019). The second depends mainly on the characteristics of the water passing through the component, in special the amount and type of abrasive particles mixed in the fluid, and the component material (FINNIE, 1960).

Thermal spray coatings have been widely studied and applied to improve the useful life of hydraulic turbines. Different processes and alloys can be used, depending on the wear phenomena and its intensity. There are a large number of publications mentioning the use of thermal spray to protect the turbine wheels from cavitation, solid particle erosion and/or corrosion, such as Vaz *et al*. (2021), Mayer *et al*. (2020), Bertuol (2020) and Pukasiewicz *et al*. (2013). One of the main advantages of thermal spray coatings consists on the elimination of welding interventions for repairing eroded areas (VAZ *et al*., 2021), which generates significant impacts to the component base material, whether metallurgically or through the induction of deformation or residual stresses. However, since the coatings act as sacrificial layers, it is essential to control the wear progress during the machine operation and to stipulate reapplications.

Regarding to erosive wear on turbine wheels, there are numerous studies and even commercial applications of hard coatings using different alloys, many of them with chromium and or tungsten carbides which have significantly higher resistance to erosion compared to carbon steel or even the martensitic stainless steels frequently used in the manufacturing of these components (BERTUOL, 2020; SHARMA, GOYAL, KAUSHAL, 2020; SANGAL; SINGHAL; SAINI, 2018; SANTA, BAENA, TORO, 2007; SUGIYAMA et al., 2005).

ASTM G40 standard defines wear as the damage to a solid surface, usually involving progressive loss of material, due to relative motion between that surface and a contacting substance or substances. The erosion phenomenon occurs in the cases where hard particles impact against a surface, carried by a flow of gas or liquid.

According to Finnie (1960), erosion mechanisms can be separated into two main types: ductile and fragile. In ductile materials, mass loss occurs due to a plastic deformation process, in which material is removed by deformation and cutting action of the abrasive particle. In case of fragile materials, the removal happens due to the encounter of cracks that radiate from the points of impact of the erosive particles.

For ductile materials, two wear mechanisms are often present: micro cutting and micro ploughing. The first causes the creation of a chip in the frontal region of the erosive particle, caused by the cutting process of the surface. In the second mechanism, the particle does not remove material from the surface, but accumulates deformed material on the margins of the cavity generated on it (JAVAHERI, PORTER e KUOKKALA, 2018). For fragile materials, the energy transferred from the solid particles to the surface causes not only deformation, but crack nucleation and propagation, resulting in the detachment of small portions from the surface (WANG, YANG, 2008).

For thermal spray coatings, the solid particle erosion resistance is related to characteristics like hardness, porosity, adhesion to the substrate and cohesion between the layer splats. The alloys that best meet these requirements are composed of a metallic matrix of chromium, cobalt, nickel, etc., with high contents of tungsten or chromium carbides (SUGIYAMA et al., 2005; KUMAR et al., 2018; THAKUR et al., 2011). The use of multi-phase materials brings the advantage of combining the strengths of different phases such high hardness, low friction or high toughness (BOUSSER, 2013), but several other alloys, with different characteristics have been studied for erosion resistant applications (SANTA, BAENA and TORO, 2007; SANTA *et al*., 2009; GREWAL *et al*., 2013; MOJENA *et al*., 2017).

The coatings applied by thermal spray are relatively thick (> 50 μm) and tend to behave, under solid particle erosion, as bulk material, without influence of thickness or substrate. However, the specific morphology of this coatings (porosity, oxides, cracks, etc.) motivates the study of the wear mechanisms as a function of the hardness level of the applied layer. In the present work, two coatings with different levels of hardness, applied by Arc Spray Process (ASP), were subject to slurry jet tests with constant parameters. The mass loss, wear rate and wear mechanisms were evaluated. Also, the influence of coating surface finishing (sanding and polishing) on the erosion resistance was investigated.

2. EXPERIMENTAL PROCEDURE

2.1 Materials

For this study two commercial alloys were selected for the coatings. Both alloys are iron based added with carbon, chromium and manganese in different proportions in order to generate hard coatings indicated for wear applications. Details of each alloy are given below and Table 1 provides the chemical compositions.

- Alloy 1 (solid wire – diam. Ø 1.6 mm): with 0.7 % (wt.) carbon and 9.8 % (wt.) chromium, it is aimed for welded coatings for demands requiring resistance to friction and abrasive wear;
- Alloy 2 (tubular wire – diam. Ø 1.6 mm): with significantly higher contents of carbon and chromium, it is an alloy specific for thermal spray and creates high hardness coatings, recommended for abrasion and erosion applications, as well as corrosion and oxidation.

Table 1: Chemical compositions of the coating alloys (% wt.).

Material	Fe	C	Si	Mn	Cr	Other (max.)
Alloy 1	Bal.	0.7	2.5	0.8	9.8	-
Alloy 2	Bal.	5.0	-	1.0	28.0	1.5

The coatings were deposited on 4.8 mm thick ASTM 1020 steel substrates, with a dimension of 100 x 40 mm.

2.2 Coatings Application

The alloys were deposited on carbon steel substrates using the ASP power source Metallisation S350(16) and gun ARC 340, at Lactec, Curitiba - PR. Table 2 exhibits the deposition parameters for Alloys 1 and 2. These parameters were selected after preliminary tests where arc stability and low porosity levels were sought. Due to the differences in chemical composition and wire format, it was expected the parameters would not be the same for each alloy. The coating application was performed robotically, using an EngeMovi seven-axis robot, Figure 1.

Table 2: Thermal spray parameters.

Material	Alloy 1	Alloy 2
Voltage (V)	33	33
Electric Current (A)	160	200
Air Pressure (MPa) [bar]	0.6 [6.0]	0.6 [6.0]
Spray Distance (mm)	130	110
Gun Velocity (mm/s)	90	
Gap (1) (mm)	18	

(1) Distance between two movements of the thermal spray gun.

Figure 1: ASP robotic coating application.

Before coating deposition, the substrates surfaces were prepared by grit blasting with #20 mesh aluminium oxide, in order to achieve Sa3 standard grade of cleanliness and roughness range of Ra 7.0 – 8.0 μm and Rt 50 – 60 μm.

2.3 Coating Surface Finishing

In order to investigate the influence of the initial surface condition on the erosion resistance, the coated samples were subjected, in addition to the as-sprayed condition, to two different finishing processes: full polishing and one step sanding.

The polishing process was carried out by sanding the coatings surfaces on #220, #320, #400, #600, #800 and #1200 grit sandpaper, followed by polishing with 3 μm diamond paste until obtaining a mirrored look of the coupons. The sanded finishing was achieved by one single step #220 grit sanding. This form of surface finishing allows a gradual assessment between the states as-sprayed and polished of the coatings and also represents an easy post-processing alternative, especially for field applications.

In order to better identify the variations studied, each coupon was named as shown in Table 3.

Table 3: Coupons identification.

Identification	Alloy	Finishing
1AS	1	As-sprayed
1SD	1	Sanded
1PO	1	Polished
2AS	2	As-sprayed
2SD	2	Sanded
2PO	2	Polished

An important information is the mass loss originated from the finishing process. So, the coupons subjected to sanding and polishing had their mass checked before and after the finishing process. These measures were carried out on an analytical balance Shimadzu AW220.

2.4 Material Characterization

To assist in evaluating of the erosive process behavior, the samples coated with and without further treatments were characterized before, during and after the erosion tests, using the following analyzes and equipment:

- Surface roughness measurement using a portable digital roughness tester Mitutoyo Surftest SJ-210;
- Cross-section morphology of coatings through metallographic preparation and analysis using an Olympus BX51M optical microscope and Stream Essentials image analysis software;
- Pores and oxides quantification by image analysis;
- Surface morphology using a scanning electron microscope (SEM) Tescan Vega 3;
- Mass analysis on a Shimadzu AW220 analytical balance;
- Vickers microhardness measurement on an EmcoTest DuraScan 20 G5, with 0,2 kg load.

For the cross-section morphology analysis, the samples were prepared following the steps: cutting in an Arotec Arocor 100 metallographic cutting machine; hot mounting in an Arotec PRE-30Mi press; sanding in #220, #320, #400, #600, #800 e #1200 sandpaper and polishing with 3 μm and 1 μm diamond paste.

The microhardness measurement was executed with nine indentations divided in three profiles of three points along the coatings cross-sections. Figure 2 illustrates the indentations distribution.

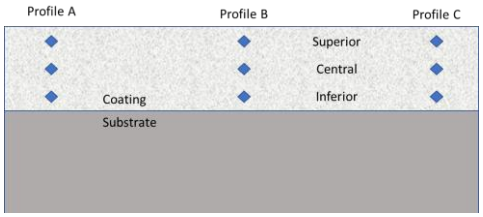

Figure 2: Microhardness indentations distribution along the coating cross-section.

2.5 Slurry Jet Test

In order to investigate the coatings response to the erosive wear, slurry jet tests were carried out using the equipment DUCOM Slurry Jet Tester, installed at campus Ponta Grossa of Federal Technological University of Paraná (UTFPR-PG). This equipment produces a water jet mixed with an abrasive media – in this case sand – which is pointed against the surface of the tested material. The jet speed, abrasive feed rate and type and jet incidence angle on the surface are the factors that can be set in this test. The Figure 3 shows the slurry jet equipment. Table 4 indicates the test parameters.

Figure 3: DUCOM Slurry jet equipment.

Table 4: Slurry jet test parameters.

Parameters	Set-up
Jet incidence angle	90 °
Abrasive	Sand 300 (200 – 400 μm)

Parameters	Set-up
Nozzle diameter	4.0 mm
Abrasive flow	1790 g/min (30 rpm)
Jet velocity	25.5 m/s (750 rpm)
Distance nozzle/surface	50 mm
Test periods	1, 2, 3 and 4 min

The required dimensions for the slurry jet coupons are 40 x 25 mm. Thus, the coated samples were cut to obtain this geometry. The mass loss during the tests was verified after each test period, using the same analytical balance specified in topic 2.4. In order to avoid errors during the mass analysis due to the presence of moisture or embedded abrasive particles on the surface, before this step each specimen was cleaned in an ultrasonic vat, immersed in absolute ethyl alcohol, for five minutes. Afterwards, the specimens were dried with air heat blower.

3. RESULTS AND DISCUSSION

3.1 Coatings Characterization – As-sprayed

Figure 4 exhibits the cross-section morphology of the coatings from Alloy 1 and Alloy 2. Both coatings presented usual aspect for ASP deposition, with flat lamellae of the metallic phase surrounded by oxide films and also the presence of pores. Visually, the Alloy 2 coating is slightly denser, but unlike Alloy 1, it is possible to observe the presence of small cracks growing vertically across the lamellae. Both coatings also present rounded particles, which may be those partially melted during the application or melted particles that solidified before the impact against the surface. These were named “PMP/PSP” or Partially Melted Particles / Previously Solidified Particles.

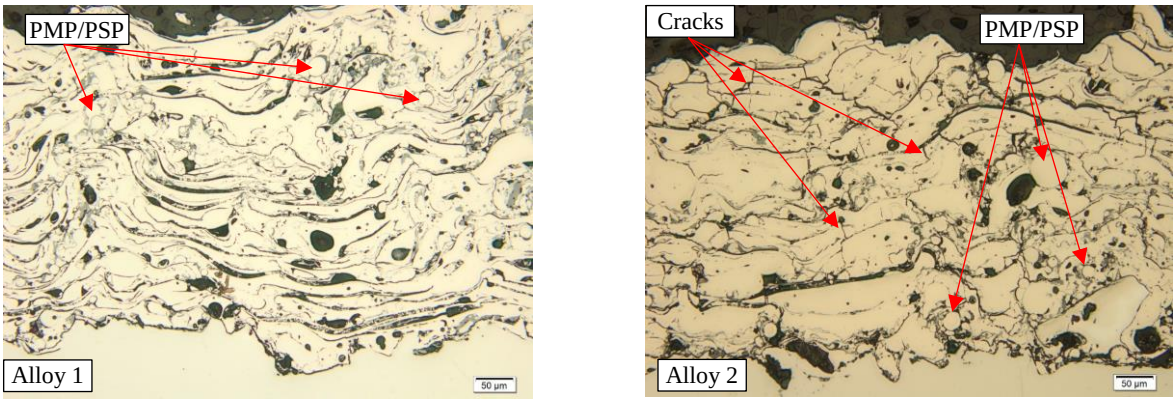

Figure 4: Cross-section morphology of Alloy 1 coating and Alloy 2 coating (scale 50 µm).

Table 5 shows the results for the measures of oxides and porosity of the coatings. As commented earlier, the Alloy 2 coating presented slightly lower levels of oxides and pores compared with Alloy 1.

Table 5: Pores and oxides results.

Coating	Measure	% Pores	% Oxides
Alloy 1	1	4.98	15.38
	2	3.88	24.21
	3	4.31	16.48
	Average	4.39	18.69
	Std. Dev.	0.55	4.81
Alloy 2	1	1.60	14.78
	2	3.51	15.17
	3	2.44	15.29
	Average	2.52	15.08
	Std. Dev.	0.96	0.27

The microhardness results are given at Table 6, considering the indentations positions detailed in topic 2.4. It is possible to observe the significant higher hardness of Alloy 2. This was expected due to the high levels of carbon and chromium in this same alloy. The metallurgical phases and constituents of each coating have not been evaluated, but

possibly the amount of such elements allows the formation of chromium carbides in the deposited layer. This would also justify the variation on the hardness values, which depends on the presence or absence of carbide at the measurement point.

Table 6: Microhardness results (HV0,2).

Coating	**Alloy 1**			**Alloy 2**		
Profile	A	B	C	A	B	C
Superior	291	309	495	623	840	1163
Central	408	396	406	828	631	783
Inferior	273	321	512	1182	849	1436
General Average	379			926		
Std. Deviation	82			259		

3.2 Slury Jet Test Results – As-sprayed

Figure 5 shows the graph of accumulated mass loss for Alloys 1 and 2 coatings, without any surface post treatment. Since the densities of each coating are similar (5,6 mg/mm³ for Alloy 1 and 5,7 mg/mm³ for Alloy 2), the results are given in mass loss – not in volume loss. The curves indicate that the wear in Alloy 2 was slightly higher in comparison with Alloy 1, considering the test parameters used.

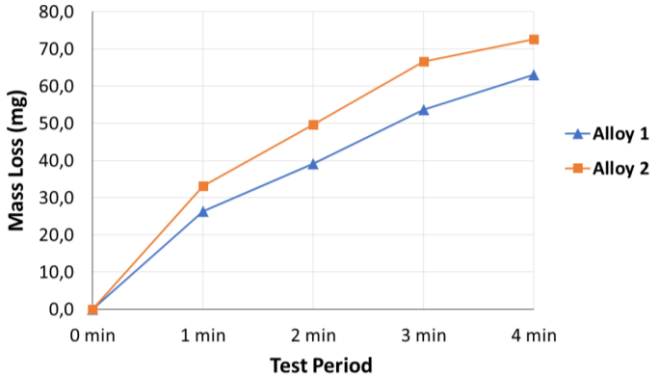

Figure 5: Accumulated mass loss of “as-sprayed” coatings.

Figure 6 exhibits the erosion rate, in “mg/min”, for each minute of the tests. The values in this graph were obtained by dividing the accumulated mass loss at a given moment by the total elapsed time (in minutes) until that moment. The graph shows that the more severe wear occurs during the first minute of test. Also, it is noticed that the difference between the two alloys is more pronounced during this same period. After that, the rates values are very similar and in the fourth minute there is an inversion of behaviour, with Alloy 2 presenting the lower erosion rate.

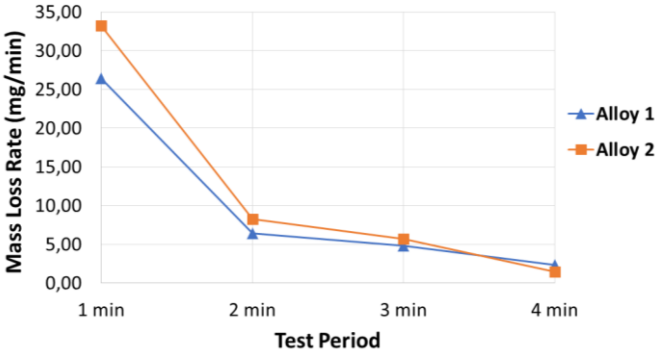

Figure 6: Erosion rate for each minute of test of “as-sprayed” coatings.

The slurry jet test results for the as-sprayed coatings indicate that, under the conditions applied, the higher hardened and lower porosity of Alloy 2 coating was not reflected in better wear resistance. This result is predictable if we consider literature information that indicates higher wear rates for fragile materials when the erosive jet angle is 90° (HUTCHINGS and SHIPWAY, 2017; JAVAHERI, PORTER and KUOKKALA, 2018).

Figure 7 exhibits SEM images from the surfaces of Alloy 1 and Alloy 2 coatings, as-sprayed, before the erosion tests. It is possible to observe the coatings splats (smooth regions), in addition to splashes (small spherical particles) and PMP/PSP (large spherical particles), which are bonded to the splats through very small contact areas. Therefore, splashes and PMP/PSP are less adherent to the coating, and easily detachable during the erosive process. This explains the higher erosion rates in the first minute of testing, when these particles are directly exposed to the erodent flow.

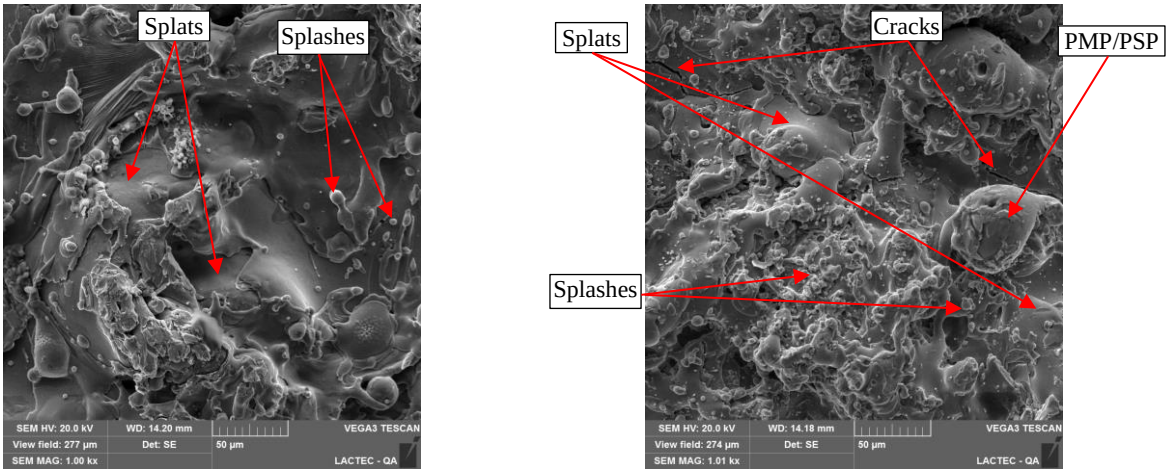

Figure 7: Surface aspect of as-sprayed Alloy 1 (left side) and Alloy 2 (right side) coatings (scale: 50 µm).

On the Alloy 2 coating, it is also possible to observe the cracks already identified on the cross-section analysis. Furthermore, compared to the Alloy 1, it presents a more heterogeneous surface, with significant presence of splashes. Cracks and splashes improved the material detachment during the erosion tests, leading to higher mass loss. Grewal *et al*. (2013) also found a similar result in nickel coatings with the addition of alumina (Al_2O_3), applied by a high-speed flame process. The authors found better wear resistance for the alloy with the addition of 40% wt. of alumina. For the condition with 70% wt. alumina and higher hardness, the wear rate was more accentuated. The justification given in this case was a better combination of hardness and fracture toughness, the latter being higher for the 40% Al_2O_3 alloy.

After the second minute of testing, the wear rates of both alloys were similar, but the way of material removal was different. Figure 8 shows the coating surface of Alloy 1 after the 4 minutes of test. It is possible to notice the presence of plastic deformation, microcutting and microploughing marks. These three types of marks are common to wear processes, especially for ductile materials, being cited by several authors, such as Javaheri, Porter and Kuokkala (2018), More, Bhatt and Menghani (2017), Grewal *et al*. (2013) e Santa, Baena and Toro (2007).

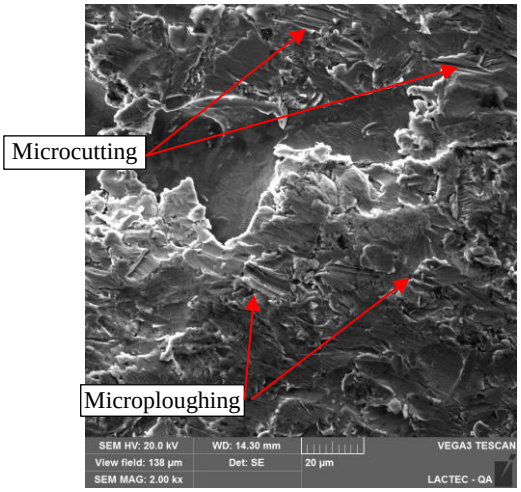

Figure 8: Alloy 1 coating surface after 4 minutes of slurry jet test (scale 20 µm).

The microscopic aspect of the worn region on the Alloy 2 coating after the 4 minutes of test is shown in Figure 9. Microcutting and microploughing marks are also present, but less evident compared to the other material. However, fracture regions with a fragile appearance are clearly observed, in special at the interfaces between the splats. This indicates the occurrence of wear mechanisms expected for brittle materials: microcracking or chipping.

3.3 Slury Jet Test Results – Surface Finishing

The accumulated mass loss curves of the coatings after surface finishing – sanding and polishing – is given in Figure 9. Again, Alloy 1 presented the better wear resistance, with the sanded surface performing better the polished one. The sanding also provided better results for Alloy 2.

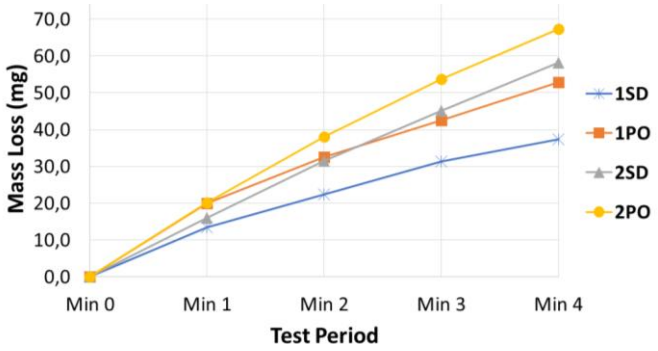

Figure 9: Accumulated mass loss of finished (sanding and polishing) coatings.

The curves for erosion rates per minute, shown in Figure 10, once again indicate higher values for the first minute of test, but on a significant lower scale compared to the as-sprayed coatings – 26 to 33 mg/min for as-sprayed condition and 16 to 20 mg/min for finished conditions. This fact could confirm that the presence of low adherence particles is responsible for a higher wear rate ate the beginning of the tests. However, the fact that there are still higher initial erosion rates, especially in polished surfaces, indicates that other factors may be influencing the wear resistance during the first minutes of the erosive process.

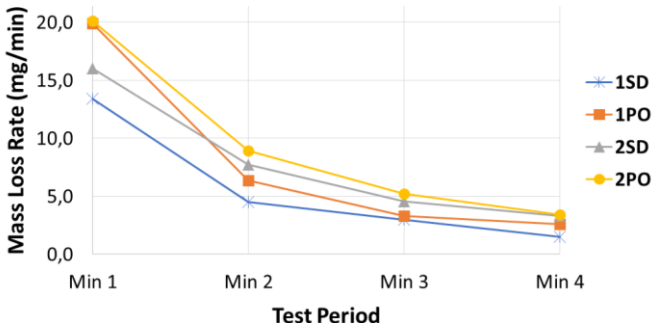

Figure 10: Erosion rate for finished (sanding and polishing) coatings.

The analyses of eroded surfaces in SEM, after the full tests, confirm that there is no change in the wear mechanisms after the initial minute. Figure 10 exposes the worn surfaces of the finished coatings, with Alloy 1 presenting greater plastic deformation besides microcutting and microploughing marks and Alloy 2 showing cracks and fragile fractures marks at the interfaces between splats.

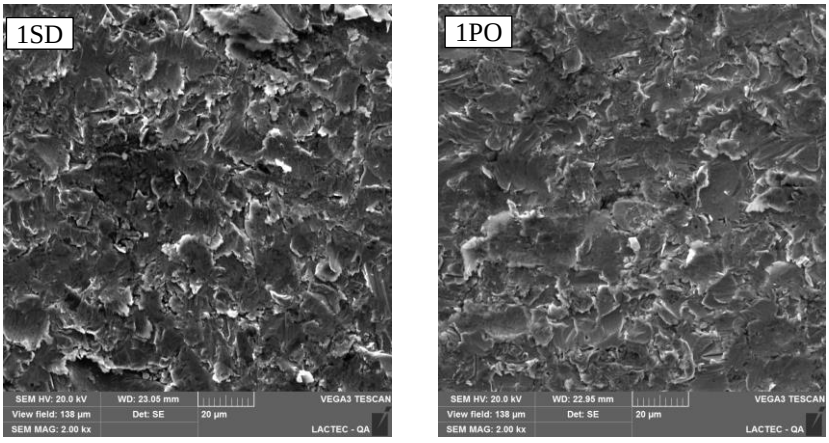

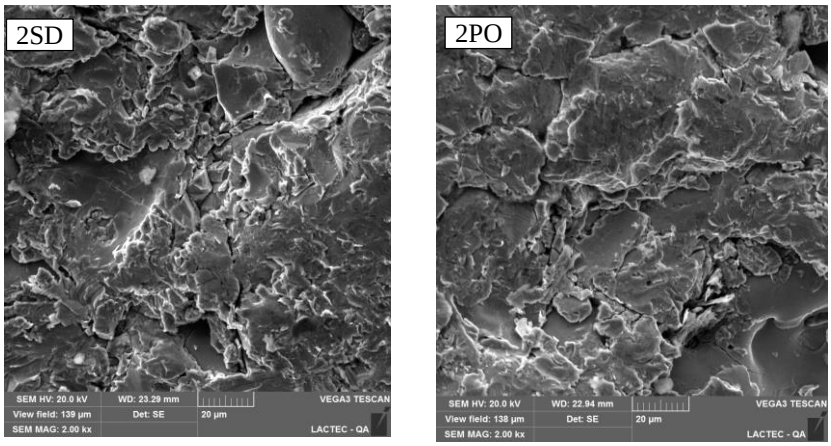

Figure 11: Eroded surfaces of coating finished with sanding or polishing (scale 20 µm).

The reduction in the initial erosion rates due to the sanding and polishing processes is interesting. However, the impact generated in the coatings by the finishing process itself must be considered, once it also removes material from the layer. Figure 12 displays again the accumulated mass loss curves, but now considering the mass variation caused by the surface treatment itself (calculated in function of the same area affected by the slurry jet test). It is clear that both polishing and simple sanding lead to a very high initial mass loss (moment zero). Thus, considering the mass loss after the 4 minutes, sanding and polishing post treatments are not advantageous.

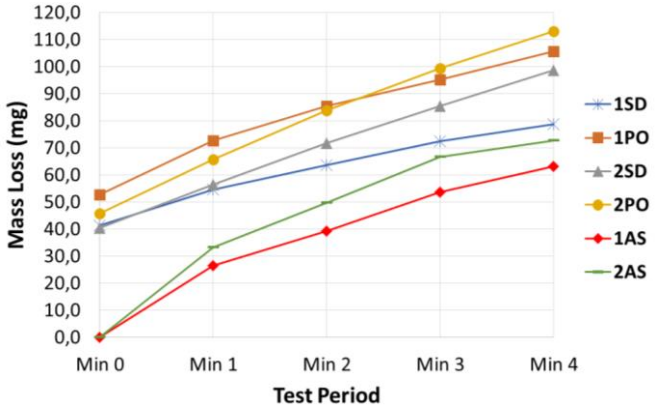

Figure 12: Accumulated mass loss considering the loss created by the finishing processes.

4. CONCLUSION

The hardness of the coatings obtained by ASP thermal spray influenced the results of slurry jet tests and the wear mechanisms acting on the materials during the tests. As expected for bulk material, considering erosive jet angle of 90 °, the coating with lower hardness and higher toughness presented reduced mass loss and wear rate compared to the harder and more fragile coating. Microcutting and microploughing mechanisms were dominant in the lower hardness coating, while microcracking and chipping were more intense on the harder layers. The finishing treatments of the coatings, simple sanding or polishing, reduced the initial wear rates, but more studies must be carried out to better understand the factors leading to a higher wear rate at the first moment of test and the higher mass loss of polished surfaces compared to the sanded ones. Finally, despite the reductions shown in wear rates, considering the loss of mass generated by the finishing processes themselves, their adoption is not advantageous for an increase in the useful life of the coatings.

5. ACKNOWLEDGEMENTS

The authors thank the Institute of Technology for Development – Lactec, UTFPR-PG (Federal Technological University of Paraná – Campus Ponta Grossa) and UFPR (Federal University of Paraná) for the support and availability of the laboratories and material necessary for the studies.

6. REFERENCES

ANEEL - Agência Nacional de Energia Elétrica. Matriz por Origem de Combustível. 2021. Disponível em: https://bityli.com/ObWtP. Acesso em: 20 fev. 2021.

ASTM INTERNATIONAL. G 40: Standard Terminology Relating to Wear and Erosion. West Conshohocken: ASTM International, 2017. 8 p.

BERTUOL, K. Estudo do Efeito Sinérgico Cavitação/Erosão em Revestimentos de Carboneto de Cromo e Tungstênio Depositados por Aspersão Térmica de Alta Velocidade. 2020. 123 f. Dissertação (Mestrado) - Curso de Engenharia Mecânica, Universidade Tecnológica Federal do Paraná, Ponta Grossa, 2020.

BOUSSER, E. Solid Particle Erosion Mechanisms Of Protective Coatings For Aerospace Applications. 2013. 215 f. Tese (Doutorado) - Département de Génie Physique, Université de Montréal, Montreal, 2013.

MOURA, A. P.; MOURA, A. A. F.; ROCHA, E. P.. Engenharia de Sistemas de Potência: geração hidroelétrica e eolioelétrica. Fortaleza: Edições UFC, 2019.

FINNIE, Iain. Erosion of surfaces by solid particles. *Wear*, [S.L.], v. 3, n. 2, p. 87-103, mar. 1960. Elsevier BV.

GREWAL, H.s.; ARORA, H.s.; AGRAWAL, Anupam; SINGH, H.; MUKHERJEE, S.. Slurry Erosion of Thermal Spray Coatings: effect of sand concentration. *Procedia Engineering*, [S.L.], v. 68, p. 484-490, 2013. Elsevier BV.

HUTCHINGS, I.; SHIPWAY, P.. Tribology: friction and wear of engineering materials. 2. ed. Oxford: Elsevier, 2017.

JAVAHERI, V.; PORTER, D.; KUOKKALA, V.. Slurry erosion of steel – Review of tests, mechanisms and materials. *Wear*, [S.L.], v. 408-409, p. 248-273, ago. 2018. Elsevier BV.

KUMAR, H.; CHITTOSIYA, C.; SHUKLA, V. N. HVOF Sprayed WC Based Cermet Coating for Mitigation of Cavitation, Erosion & Abrasion in Hydro Turbine Blade. *Materials Today: Proceedings*, v. 5, n. 2, p. 6413–6420, 2018.

MAYER, A. R.; BERTUOL, K.; SIQUEIRA, I. B.A.F.; CHICOSKI, A.; VÁZ, R. F.; SOUSA, M. J. de; PUKASIEWICZ, A. G. M.. Evaluation of cavitation/corrosion synergy of the Cr3C2-25NiCr coating deposited by HVOF process. *Ultrasonics Sonochemistry*, [S.L.], v. 69, p. 105271-105280, dez. 2020. Elsevier BV.

MOJENA, M. Á. R.; OROZCO, M. S.; FALS, H. C.; ZAMORA, R. S.; LIMA, C. R. C. A comparative study on slurry erosion behavior of HVOF sprayed coatings. Dyna, [S.L.], v. 84, n. 202, p. 239-246, 1 jul. 2017. Universidad Nacional de Colombia.

MORE, S.R.; BHATT, D.V.; MENGHANI, J.V.. Study of the Parametric Performance of Solid Particle Erosion Wear under the Slurry Pot Test Rig. Tribology In Industry, [S.L.], v. 39, n. 4, p. 471-481, dez. 2017. Faculty of Engineering, University of Kragujevac.

MULLER, G. de M.. Despacho de Máquinas e Geração de Usina Hidrelétrica Individualizada Utilizando Algoritmos Genéticos. 2010. 168 f. Dissertação (Mestrado) - Curso de Engenharia Elétrica, Universidade Federal do Rio de Janeiro, Rio de Janeiro, 2010.

PUKASIEWICZ, A. G. M.; CAPRA, A. R.; VAZ, R. F.. Cavitation Resistance Of Asp Coatings, Ultrasonic Testings And Francis Runner Field Performance Comparison. In: Materials Science And Technology (MS&T), 13., 2013, Montreal. *Proceedings: Ms&t13*, 2013. p. 799-805.

SANGAL, S.; SINGHAL, M. K.; SAINI, R. P.. Hydro-abrasive erosion in hydro turbines: a review. International *Journal Of Green Energy*, [S.L.], v. 15, n. 4, p. 232-253, 12 fev. 2018. Informa UK Limited.

SANTA, J.F.; BAENA, J.C.; TORO, A.. Slurry erosion of thermal spray coatings and stainless steels for hydraulic machinery. *Wear*, [S.L.], v. 263, n. 1-6, p. 258-264, set. 2007. Elsevier BV.

SANTA, J.F.; ESPITIA, L.A.; BLANCO, J.A.; ROMO, S.A.; TORO, A.. Slurry and cavitation erosion resistance of thermal spray coatings. *Wear*, [S.L.], v. 267, n. 1-4, p. 160-167, jun. 2009. Elsevier BV.

SHARMA, M.; GOYAL, D. K.; KAUSHAL, G.. Tribological Investigation of HVOF Sprayed Coated Turbine Steel under Varied Operating Conditions. *Materials Today: Proceedings*, [S. L.], v. 24, p. 869-879, 2020.

SUGIYAMA, K.; NAKAHAMA, S.; HATTORI, S.; NAKANO, K. Slurry wear and cavitation erosion of thermal-sprayed cermets. *Wear*, v. 258, n. 5–6, p. 768–775, 2005.

THAKUR, L.; ARORA, N.; JAYAGANTHAN, R.; SOOD, R. An investigation on erosion behavior of HVOF sprayed WC-CoCr coatings. *Applied Surface Science*, v. 258, n. 3, p. 1225–1234, 2011.

VAZ, R. F.; SUCHARSKI, G. B.; CHICOSKI, A.; SIQUEIRA, I. B. A. F.; TRISTANTE, R.; PUKASIEWICZ, A. G. M.. Comparison of FeMnCrSi Cavitation Resistance Coatings Deposited by Twin-Wire Electric Arc and High-Velocity Oxy-Fuel Processes. *Journal Of Thermal Spray Technology*, [S.L.], 24 jan. 2021. Springer Science and Business Media LLC.

WANG, Y.; YANG, Z.. Finite element model of erosive wear on ductile and brittle materials. *Wear*, [S.L.], v. 265, n. 5-6, p. 871-878, ago. 2008. Elsevier BV. http://dx.doi.org/10.1016/j.wear.2008.01.014.

7. RESPONSIBILITY NOTICE

The authors are the only responsible for the printed material included in this paper.